

Quantum Mixed-State Self-Attention Network

Fu Chen^{a,b}, Qinglin Zhao^{a,*}, Li Feng^a, Chuangtao Chen^a, Yangbin Lin^c,
Jianhong Lin^d

^a*Faculty of Innovation Engineering, Macau University of Science and
Technology, Macau, 351100, China*

^b*New Engineering Industry College, Putian University, Putian, 361021, China*

^c*Computer Engineering College, Jimei University, Xiamen, 999078, China*

^d*Mechanical, Electrical and Information Engineering College, Putian
University, Putian, 351100, China*

Abstract

The rapid advancement of quantum computing has increasingly highlighted its potential in the realm of machine learning, particularly in the context of natural language processing (NLP) tasks. Quantum machine learning (QML) leverages the unique capabilities of quantum computing to offer novel perspectives and methodologies for complex data processing and pattern recognition challenges. This paper introduces a novel Quantum Mixed-State Attention Network (QMSAN), which integrates the principles of quantum computing with self-attention networks, to enhance the efficiency and effectiveness in handling NLP tasks. QMSAN model employs a quantum attention mechanism based on mixed states, enabling efficient direct estimation of similarity between queries and keys within the quantum domain, leading to more effective attention coefficients acquisition. Additionally, we propose an innovative quantum positional encoding scheme, implemented through fixed quantum gates within the quantum circuit, to enhance the model's accuracy. Experimental validation on various datasets demonstrates that QMSAN model outperforms existing quantum and classical models in text classification, achieving significant performance improvements. QMSAN model not only significantly reduces the number of parameters but also exceeds classical self-attention networks in performance, showcasing its strong capability in data representation and information extraction. Furthermore, our study

*Co-corresponding author

Email address: qlzhao@must.edu.mo (Qinglin Zhao)

investigates the model’s robustness in different quantum noise environments, showing that QMSAN possesses commendable robustness to low noise.

Keywords: Quantum machine learning, Self-attention mechanism, Quantum self-attention mechanism, Text categorization

1. Introduction

Over the past few decades, the rapid advancement of quantum computing has revolutionized various fields by leveraging the principles of quantum mechanics to achieve unprecedented computational speed and efficiency, particularly in biology[1], cryptography[2], and communication technology[3]. This advancement has led to the merging of quantum methods with machine learning, particularly in Quantum Machine Learning (QML). This emerging field combines the principles of quantum computing with traditional machine learning techniques to tackle complex challenges in data processing and pattern recognition[4, 5, 6, 7]. Initially, the field of Natural Language Processing (NLP) has also seen significant advancements through the development of deep learning models like Convolutional Neural Networks (CNNs)[8] and Recurrent Neural Networks (RNNs)[9], which have dramatically improved tasks such as text classification[10, 11], sentiment analysis[12, 13], and machine translation[14, 15]. More recently, the introduction of Transformer models[16] and OpenAI’s GPT series[17, 18] have further extended NLP capabilities, enabling models to generate complex text and interact naturally with humans[19, 20], even extending their creativity to composing music[21], crafting literature[22], and developing software[23]. However, with the growth of model size and data volume, classical deep learning methods face huge demands for computational resources and challenges in energy efficiency [24, 25, 26].

Quantum computing provides a new direction for the field of Natural Language Processing. Quantum computers are expected to achieve quantum advantage[27, 28], which can be reflected in sample complexity or time complexity [29]. The core characteristics of quantum computing, such as quantum superposition and quantum entanglement, offer new possibilities for representing and processing the high-dimensional data of natural language, allowing for the representation of a large number of words and sentences in the high-dimensional Hilbert space [30, 31], and capturing complex relationships and semantic information between words. Moreover, quantum algo-

gorithms can achieve faster processing speeds than classical algorithms in some cases[32, 33], which is significant for accelerating the training and inference processes of NLP tasks. Through Quantum Natural Language Processing (QNLP), researchers explore the use of the unique advantages of quantum computing to process language data and perform NLP tasks[34], which has inspired some exploratory work.

Up to now, in 2023, Li et al. proposed a fully quantum learning model, QRNN [35], which stacks recurrent blocks in an alternating manner to reduce the algorithm’s requirements for the coherence time of quantum devices. In 2022, SYC Chen et al. proposed a hybrid quantum-classical model, QLSTM [36], which extends the classical Long Short-Term Memory (LSTM) model to the quantum domain, replacing some classical neural networks in the LSTM unit with Variational Quantum Circuit (VQC) to construct a more efficient model. However, these quantum versions of RNN and LSTM models have the same problems as classical neural networks: they often struggle to capture long-distance dependencies and have limited capabilities in handling complex problems. In 2017, Niu et al. proposed a more efficient, parameter-free model combining quantum attention with LSTM based on weak measurement in quantum mechanics[37], which has better sentence modeling performance. However, this method mainly focuses on some physical principles of quantum mechanics and does not involve specific quantum circuit design.

A more effective quantum self-attention network is the Quantum Self-Attention Neural network (QSANN) model proposed by Baidu’s team in 2022, which uses Gaussian projection quantum self-attention for text classification [38]. This model can explore the correlations between words in the high-dimensional quantum feature space. However, when processing quantum queries and keys, the model converts them into classical data through observables to calculate similarity. This process involves information loss and reduces the model’s ability to leverage the advantages of quantum computing. In 2022, the Quantum Self-Attention Network (QSAN) model proposed by Zhao et al. [39] uses Quantum Logic Similarity (QLS) to prevent measurement from obtaining inner products and Quantum Bit Self-Attention Score Matrix (QBSASM) to generate a density matrix that effectively reflects the output attention distribution, thereby enhancing the model’s information extraction capability. In 2023, Zhao et al. proposed the Quantum Kernel Self-Attention Network (QKSAN) model[40], which combines the data representation advantages of quantum kernel methods with the efficient infor-

mation extraction capability of self-attention mechanism, providing a larger and more complex data representation space. Although these two methods compute the similarity of quantum queries and keys at the quantum level, they are limited to the pure state level and rely on the unitary transformation of quantum circuits, resulting in limited expressive power. Moreover, up to now, these implemented quantum self-attention networks have not yet introduced position information, The potential of the models has not been fully realized.

To overcome the issues mentioned above and explore the advantages of quantum computing in improving classical self-attention network models for more effective attention results, we propose a novel model, called Quantum Mixed-State Attention Network (QMSAN) model. This model is based on trainable quantum embeddings, quantum attention coefficients based on mixed states, and non-trainable quantum positional information embedding. To evaluate the performance of our model, we conducted numerical experiments with various datasets. Compared to classical self-attention networks, our model significantly reduces the number of parameters under the same input sequence conditions. For the self-attention network model in the same quantum domain, our model demonstrates superior performance, indicating that QMSAN model has stronger data representation and information extraction capabilities. The main contributions of this paper are summarized as follows:

- We propose a novel quantum attention coefficients calculation mechanism based on mixed states. In the context of quantum computing, the representations of queries and keys are not conventional pure-state qubits but are realized through quantum mixed states. This allows the model to capture richer information and intrinsic data correlations. The similarity between queries and keys is directly estimated at the quantum level without degrading the quantum information of queries and keys into classical information for processing. This calculation process not only maintains the efficiency and parallelism of quantum computing but also avoids the accuracy decline caused by information loss.
- Recognizing the importance of positional information in many NLP tasks, we propose a novel quantum positional encoding scheme. This scheme adopts an absolute positional encoding form without the need for additional qubits. We implement positional information encoding

by introducing additional fixed quantum gates into the quantum circuit, which avoids the extra demand for qubits while maintaining the efficiency and accuracy of encoding.

- We incorporate a trainable quantum embedding model into our model, further optimizing the implementation framework of quantum self attention networks by integrating the originally separate fixed quantum embedding and trainable quantum neural network (QNN) structures into a unified trainable quantum embedding model, exploring and verifying its application potential in quantum self-attention networks.

The rest of the paper is structured as follows: First, in Section 2, we summarize the basic theory and methods. Then, in Section 3, we elaborate on our innovative QMSAN framework and introduce its corresponding quantum circuits. The numerical simulation setup and comparison results with other attention models are presented in Section 4. Finally, Section 5 concludes the paper.

2. PRELIMINARIES

Before delving into quantum self-attention networks, it is necessary to understand a few fundamental concepts of quantum mechanics, including quantum states, and observables.

2.1. Quantum States

In quantum mechanics, the states of quantum systems are generally described in the form of pure states and mixed states. A pure state can be represented by a vector $|\psi\rangle$ in Hilbert space[41]. For a simple qubit system, its pure state can be represented as follows:

$$|\psi\rangle = \alpha |0\rangle + \beta |1\rangle \tag{1}$$

where $|0\rangle$ and $|1\rangle$ represent the two basis states of the qubit, while α and β are complex coefficients. The absolute squares of these coefficients ($|\alpha|^2$ and $|\beta|^2$) represent the probabilities of measuring the corresponding basis states, and they satisfy $|\alpha|^2 + |\beta|^2 = 1$.

Unlike pure states, which represent a quantum system in a completely determined state, mixed states describe a system that is in a probabilistic

mixture of multiple pure states. Mixed states are usually represented by a density matrix ρ :

$$\rho = \sum_i p_i |\psi_i\rangle \langle \psi_i| \quad (2)$$

where $|\psi_i\rangle$ are the pure states the system can be in, and p_i is the probability that the system is in state $|\psi_i\rangle$, satisfying $\sum_i p_i = 1$.

Quantum systems evolve through linear and unitary evolution via quantum circuits. Mathematically, a pure state $|\psi\rangle$ can evolve into another pure state $|\psi'\rangle$ through the action of a quantum gate (or quantum circuit):

$$|\psi'\rangle = U |\psi\rangle \quad (3)$$

The evolution of a mixed state is described by its density matrix, where a mixed state ρ evolves into a new mixed state ρ' as:

$$\rho' = U \rho U^\dagger \quad (4)$$

where U is a unitary matrix representing the action of the quantum gate or quantum circuit, satisfying $UU^\dagger = U^\dagger U = I$. U^\dagger is the conjugate transpose of U , and I is the identity matrix.

2.2. Observables in Quantum Mechanics

In quantum computing, a quantum system can extract computational results using observables at the final output stage of a quantum computer, converting quantum information into classical data through measurement. A projective measurement is described by an observable M , a Hermitian operator on the state space of the system being observed. Mathematically, an observable M can be represented as a combination of its eigenvalues λ_i and corresponding projection operators P_i , i.e., $M = \sum_i \lambda_i P_i$. The measurement result will randomly obtain an eigenvalue λ_i , and at the same time, the quantum state $|\phi\rangle$ will collapse to the corresponding eigenstate with probability $p(\lambda_i) = \langle \phi | P_i | \phi \rangle$. Therefore, the average value of the observable M can be expressed as:

$$\langle M \rangle = \sum_i \lambda_i \langle \phi | P_i | \phi \rangle \quad (5)$$

For mixed states, the expectation value of the observable M can be calculated using the density matrix ρ :

$$\langle M \rangle = \text{tr}(\rho M) \quad (6)$$

where $\text{tr}(\cdot)$ represents the trace operation. In this paper, we will use the observable Z where $Z = (+1)|0\rangle\langle 0| + (-1)|1\rangle\langle 1|$, for example, in a system of n qubits, the observable n for the first qubit is mathematically expressed as $Z_1 = Z \otimes I^{\otimes(n-1)}$.

3. Quantum Mixed-State Attention Network Framework

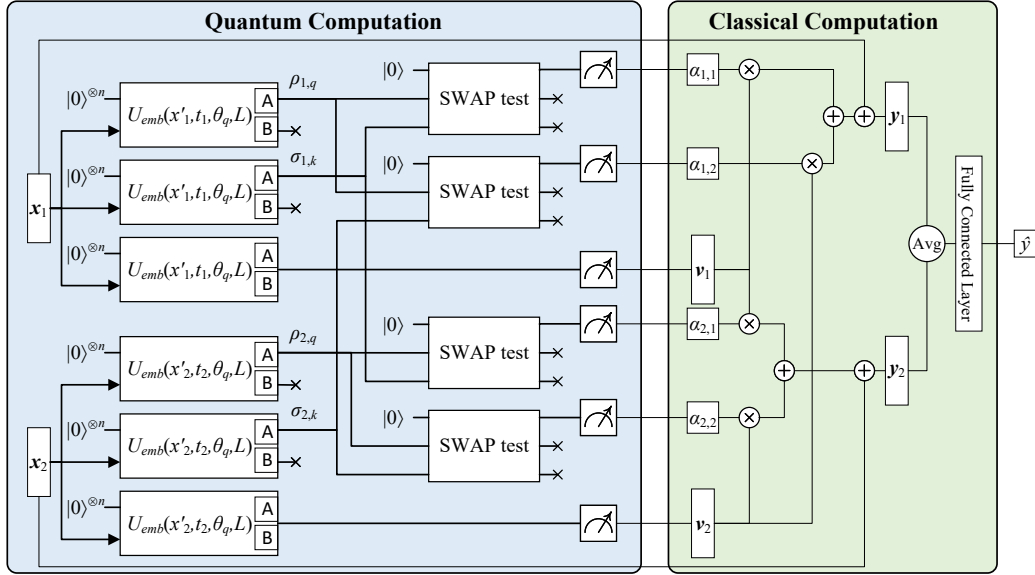


Figure 1: Quantum Mixed-State self-attention network framework.

In QMSAN model, we first transform the classical input data \mathbf{x}_s into quantum states $\rho_{s,q}$, $\sigma_{s,k}$, and $|x_{s,v}\rangle$ through three trainable Quantum Embeddings. This process involves quantum feature mapping, which directly converts classical data into quantum states. Then, we calculate the mixed-state similarity between $\rho_{s,q}$, $\sigma_{s,k}$, and measure the observable Z for $|x_{s,v}\rangle$. Afterwards, the data is fed into a classical fully connected network to complete binary prediction tasks. The architectural design of QMSAN model is illustrated in Fig. 1.

In this section, we will detail the components of the Quantum Mixed-State Self-Attention Network (QMSAN).

3.1. Quantum Mixed State Embedding

In this section, we extend the concept of quantum embeddings to include mixed state representations, providing a more general and powerful data representation framework. Mixed states offer enhanced representational power by enabling a system to encode and process a superposition of multiple quantum states simultaneously. This capability is particularly advantageous in the context of quantum self-attention mechanisms where the complexity and diversity of data relationships demand robust and flexible representation methods.

When designing a quantum self-attention network, a straightforward and natural way to calculate the similarity between queries and keys is to use the inner product:

$$\alpha_{s,j} = |\langle x_{s,q} | x_{j,k} \rangle|^2 \quad (7)$$

However, in quantum circuits, since only unitary transformations are performed, the transformation between $|x_{s,q}\rangle$ and $|x_{j,k}\rangle$ for the same number of qubits can be considered a rotation operation, as they both reside in the same Hilbert space. In contrast, in classical self-attention networks, the query vector and the key vector are:

$$\mathbf{q} = \mathbf{x}\mathbf{W}_q, \mathbf{k} = \mathbf{x}\mathbf{W}_k \quad (8)$$

where \mathbf{x} is the input vector, and W_q and W_k are the corresponding coefficients matrices. \mathbf{W}_q and \mathbf{W}_k change the direction and length of \mathbf{x} . The relationship between \mathbf{q} and \mathbf{k} involves rotation and scaling. Therefore, Ref.[38] argues that this makes it difficult for $|x_{s,q}\rangle$ to simultaneously correlate those $|x_{s,j}\rangle$ that are far away. This direct way is not optimal for calculating quantum attention coefficients.

Based on the above analysis, we propose a quantum self-attention network based on mixed states to these shortcomings. By performing partial trace operations on the pure state query and key vectors, we obtain mixed-state queries ρ_q and keys σ_k . Although this operation reduces their dimensions, it also introduces variations in the Bloch vector orientations and magnitudes within the Bloch sphere.

Following the rationale for employing mixed states, we now detail the design of the quantum embedding circuits that facilitate these states. The embedding circuit, designed to transform classical data inputs into quantum states, employs quantum feature maps followed by trainable, adaptable

variational quantum circuits, facilitating their integration into quantum self-attention mechanisms.

Typically, quantum machine learning methods focus on using fixed quantum feature maps, followed by applying a trainable, adaptable variational quantum circuit to adjust the measurement basis. This architecture, consisting of a data encoding circuit and a learnable Quantum Neural Network (QNN), is widely applied in various scenarios such as quantum convolutional neural networks [42], Quantum Recurrent Neural Networks [35], strongly entangling circuit architectures [43], and searched architectures [44, 45]. However, this approach requires careful design of the encoding circuit, as the fixed quantum feature map significantly impacts the algorithm’s generalization performance, and most computational resources are used for the QNN. Yet, Ref. [46, 47, 48] suggest that this might not be the most efficient method.

If the data is already well-mapped in Hilbert space, then subsequent tasks can be achieved with a shallow quantum classifier circuit. This is similar to the "feature extractor" in classical machine learning [49, 50], where networks are trainable with the core purpose of converting or encoding input data (such as images, text, or audio) into a new feature space. This feature space more effectively represents the key information of the data, facilitating subsequent tasks such as classification, regression, or clustering. Therefore, we can focus the adaptive training of the quantum circuit on training a trainable quantum feature map. This maps classical data into Hilbert space. We refer to this process as quantum embedding.

We introduce a repetitive iterative architecture for quantum embedding [47], as shown in Fig. 2. In classical self-attention networks, there are three parts: query, key, and value. Similarly, in our quantum self-attention network, we train three quantum embeddings. Through these embeddings, we represent classical data \mathbf{x}_s as quantum states $|x_{s,q}\rangle$, $|x_{s,k}\rangle$, and $|x_{s,v}\rangle$, where $1 \leq s \leq S$ and S represents the number of input vectors in the data sample.

Specifically, these three mappings to $|x_q\rangle$, $|x_k\rangle$, and $|x_v\rangle$ use the same ansatz structure, implemented with different parameters $\boldsymbol{\theta}_q$, $\boldsymbol{\theta}_k$, and $\boldsymbol{\theta}_v$ for query, key, and value functions, respectively. The ansatz employs single qubit and two qubit quantum gates. First, we use the single qubit gate $R_x(x_i)$ to encode the input data $\mathbf{x} = (x_1, \dots, x_N)^T$ into the quantum circuit. Then, we use the $R_{zz}(\theta_1) = e^{-i\theta_1\sigma_z \otimes \sigma_z}$ gate to entangle the qubits and add $R_y(\theta_2)$. To enhance the expressiveness of the quantum circuit, it can contain L layers of such structure. Finally, we add the single qubit gate $R_x(x_i)$ again in the last layer to encode the data. Thus, the entire circuit can be represented as

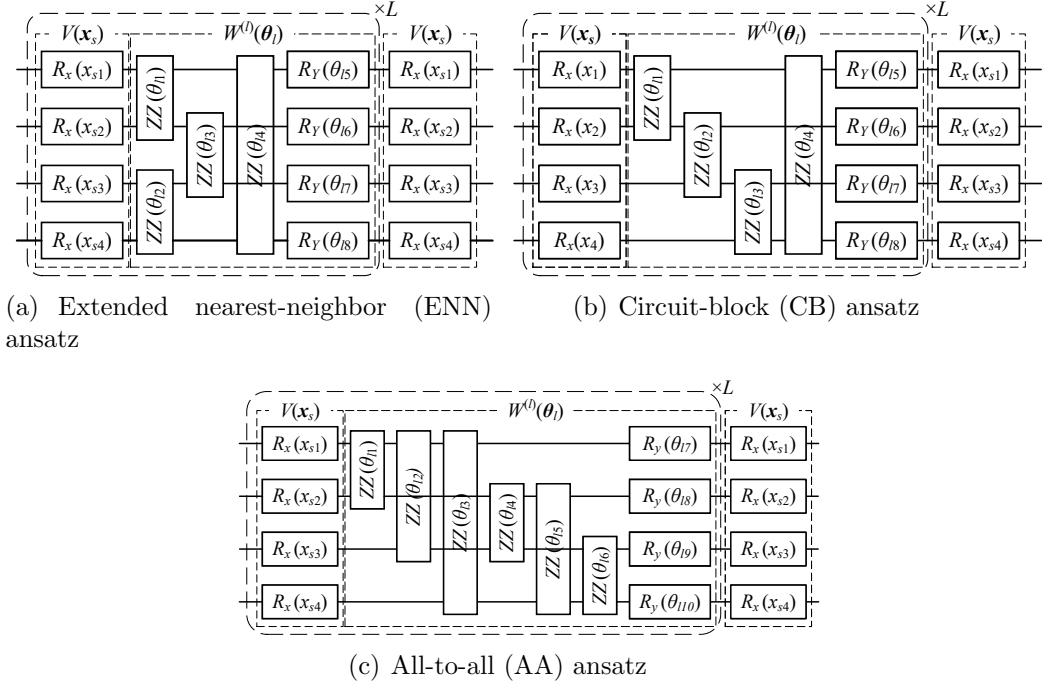


Figure 2: Three Quantum Embedding Ansatzes with Different Entanglement Layers.

$U_{emb}(\mathbf{x}, \boldsymbol{\theta})$, where \mathbf{x} is the input data and $\boldsymbol{\theta}$ are the trainable parameters. Each layer consists of a data encoding circuit block $V(\mathbf{x})$ and a trainable circuit block $W(\boldsymbol{\theta}_l)$ controlled by the trainable parameters $\boldsymbol{\theta}_l$ of each layer.

$$U_{emb}(\mathbf{x}, \boldsymbol{\theta}, L) = V(\mathbf{x}) \prod_{l=1}^L (W^{(l)}(\boldsymbol{\theta}_l) V(\mathbf{x})) \quad (9)$$

Therefore, through three trainable quantum embeddings, we embed the input data \mathbf{x}_s into three quantum states:

$$\begin{aligned} |x_{s,q}\rangle &= U_{emb}(\mathbf{x}_s, \boldsymbol{\theta}_q, L) |0\rangle^{\otimes n} \\ |x_{s,k}\rangle &= U_{emb}(\mathbf{x}_s, \boldsymbol{\theta}_k, L) |0\rangle^{\otimes n} \\ |x_{s,v}\rangle &= U_{emb}(\mathbf{x}_s, \boldsymbol{\theta}_v, L) |0\rangle^{\otimes n} \end{aligned} \quad (10)$$

For $|x_{s,q}\rangle$ and $|x_{s,k}\rangle$, they are obtained from the initial state $|0\rangle^{\otimes n}$ through the unitary transformation $U_{emb}(\mathbf{x}, \boldsymbol{\theta})$, so $|x_{s,q}\rangle$ and $|x_{s,k}\rangle$ are both pure states. To obtain the mixed states, we extract information from the first

$n/2$ -qubit subsystem A of the entire n -qubit quantum system by performing a partial trace operation on the quantum system and discarding the remaining $n/2$ -qubit subsystem B . Specifically, this operation transforms the pure states $|x_q\rangle$ and $|x_k\rangle$ of the entire system into the mixed states ρ_q and σ_k of the corresponding subsystems, respectively:

$$\begin{aligned}\rho_{s,q} &= \text{tr}_B(|x_{s,q}\rangle \langle x_{s,q}|) \\ \sigma_{s,k} &= \text{tr}_B(|x_{s,k}\rangle \langle x_{s,k}|)\end{aligned}\tag{11}$$

where $\text{tr}_B(\cdot)$ is the partial trace over system B .

The resulting states, $\rho_{s,q}$ and $\sigma_{s,k}$, when represented in the same dimensional space using Bloch vectors, exhibit discrepancies not only in vector orientation but also in vector magnitude.

3.2. Quantum Self-Attention Mechanism

Our quantum self-attention mechanism calculates the similarity of queries and keys directly within the quantum state dimensions, preserving their native quantum forms throughout the computation process until the final measurement step. This approach ensures that the entirety of quantum information is preserved, leveraging the unique properties of quantum mechanics to enhance the efficiency and accuracy of similarity calculations between the elements of the network. By maintaining the quantum information at the quantum level without converting it into classical data prematurely, our method avoids the potential loss of information typically associated with observable-based approaches. This not only prevents the degradation of quantum data fidelity but also circumvents the limitations observed in traditional methodologies where significant quantum details can be lost in the transition to classical representations.

Our approach to computing attention coefficients for mixed state queries and keys is inspired by the Hilbert-Schmidt distance. The Hilbert-Schmidt distance is an important distance metric in quantum information theory [51]. It can be measured and optimized with a small quantum circuit, making it significant for near-term quantum computing [47]. Its definition is as follows:

$$D_{\text{HS}}(\rho, \sigma) = \text{tr}((\rho - \sigma)^2)\tag{12}$$

Expanding the equation above results in three distinct terms: $\text{tr}(\rho\sigma)$, $\text{tr}(\sigma^2)$, and $\text{tr}(\rho^2)$ [47]. The term $\text{tr}(\rho\sigma)$ quantifies the distance between two ensembles in Hilbert space through the overlap between clusters; a value of

$\text{tr}(\rho\sigma) = 1$ suggests that the ensembles are formed from identical pure states, whereas $\text{tr}(\rho\sigma) = 0$ indicates orthogonality among all embedded data points. The 'purity' terms $\text{tr}(\rho^2)$ and $\text{tr}(\sigma^2)$ assess the overlap within clusters. In the quantum self-attention network, since we are more concerned with the similarity between queries and keys, we omit $\text{tr}(\sigma^2)$ and $\text{tr}(\rho^2)$, ultimately using only $\text{tr}(\rho\sigma)$ as the method for calculating the similarity between queries and keys in the quantum self-attention network.

We define quantum self-attention coefficient between the s -th and j -th mixed states, computed from the corresponding query and key parts:

$$\alpha_{s,j} = \text{tr}(\rho_{s,q}\sigma_{j,k}) \quad (13)$$

The above equation can be easily implemented by the SWAP test quantum circuit [52, 53], as shown in Fig. 3. Following this, we outline the basic principles behind the circuit's implementation of Equation 13.

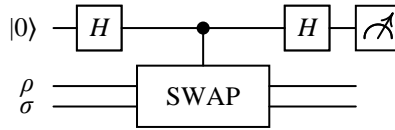


Figure 3: Quantum circuit implementing the SWAP test.

Suppose we have a pair of mixed states ρ and σ of n qubits, with $\rho = \sum_i p_i |e_i\rangle \langle e_i|$ and $\sigma = \sum_i q_i |f_i\rangle \langle f_i|$ decomposed using their respective orthogonal bases $|e_i\rangle$ and $|f_i\rangle$. If we perform a measurement on the auxiliary qubit and obtain the result $|0\rangle$, the SWAP test passes, otherwise it fails. The probability of the mixed state $\rho \otimes \sigma$ passing the SWAP test is [54]:

$$p(|0\rangle) = \sum_i \sum_j p_i q_j \left(\frac{1}{2} + \frac{|\langle e_i | f_j \rangle|^2}{2} \right) = \frac{1}{2} + \frac{1}{2} \text{tr}(\rho\sigma) \quad (14)$$

Therefore, we use the SWAP test quantum circuit to implement the calculation of quantum self-attention coefficients between queries and keys. This can effectively estimate the closeness of two mixed states. If the two mixed states are identical, $\rho = \sigma$, the test always passes with $p = 1$. When the states are different, the finite probability p of passing the test depends on the similarity $\text{tr}(\rho\sigma)$ between the two states; the closer they are, the greater the probability of passing the test. The output solution process is described

in matrix form, and coefficients matrix can be represented as

$$\mathbf{C} = \begin{bmatrix} \tilde{\alpha}_{1,1} & \tilde{\alpha}_{1,2} & \cdots & \tilde{\alpha}_{1,S} \\ \tilde{\alpha}_{2,1} & \tilde{\alpha}_{2,2} & \cdots & \tilde{\alpha}_{2,S} \\ \vdots & \vdots & \ddots & \vdots \\ \tilde{\alpha}_{S,1} & \tilde{\alpha}_{S,2} & \cdots & \tilde{\alpha}_{S,S} \end{bmatrix} \quad (15)$$

where $\tilde{\alpha}_{s,j}$ represents the normalized quantum self-attention coefficients:

$$\tilde{\alpha}_{s,j} = \frac{\alpha_{s,j}}{\sum_{m=1}^S \alpha_{s,m}} \quad (16)$$

For the value part, we use an n -dimensional vector to represent it, with the observable Z measured for each qubit, resulting in a vector with the same dimension as the number of qubits.

$$\mathbf{v}_s = [\langle Z_1 \rangle_s \quad \langle Z_2 \rangle_s \quad \cdots \quad \langle Z_n \rangle_s]^\top \quad (17)$$

Finally, the classical form of the output y_s can be calculated by the following formula. We adopt the structure of a residual network to design the output to prevent the network from degeneration:

$$\mathbf{y}_s = \mathbf{x}_s + \sum_{j=1}^S \mathbf{C}_{s,j} \cdot \mathbf{v}_j \quad (18)$$

3.3. Quantum Position Encoding

Our QMSAN, similar to classical self-attention networks, can model the relationships among tokens in a sequence and capture the contextual representation of a given token, with an outstanding ability to capture long-range dependencies. However, self-attention networks have an inherent limitation in that they cannot capture the sequential order of the input tokens [55, 56, 57]. Therefore, to enable the model to exploit the order of tokens, we must inject some information about the position of tokens in the sequence.

For quantum position encoding, using the entanglement property of quantum systems for encoding is an effective strategy. Ref.[58] proposes a method in which classical positional information can be encoded onto one or more additional qubits through quantum embedding. Subsequently, a trainable QNN circuit fully entangles the qubits with positional information with the data qubits, allowing the output quantum state of the entire system to contain

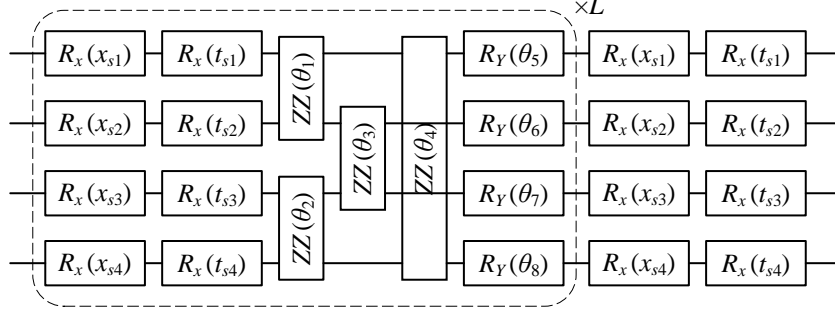


Figure 4: Introducing Positional Encoding in Quantum Embedding Circuits.

positional information. However, this method requires additional quantum qubits resources. In this study, we adopt a different approach, as shown in Fig. 4. We designed a quantum circuit that eliminates the need for auxiliary qubits by sacrificing circuit depth, thereby saving quantum qubits resources. We introduce more quantum gate operations into the quantum circuit to achieve effective encoding of positional information.

Inspired by the Ref.[16], we introduce the sinusoidal positional encoding into the quantum circuit. In classical sinusoidal positional encoding, the values of the position vector corresponding to the position at even and odd positions are:

$$\begin{aligned} PE_{s,2i} &= \sin(s/10000^{2i/d_{\text{model}}}) \\ PE_{s,2i+1} &= \cos(s/10000^{2i/d_{\text{model}}}) \end{aligned} \quad (19)$$

where s is the position, i is the dimension, and the positional encoding has the same dimension d_{model} as the embedding.

We scale the positional encoding data to the range $[0, 2\pi]$:

$$\mathbf{t}_s = \frac{\mathbf{PE}_s - PE_{\min}}{PE_{\max} - PE_{\min}} \times 2\pi \quad (20)$$

For the input data \mathbf{x} , we scale its range to $[0, \pi]$:

$$\mathbf{x}'_s = \frac{\mathbf{x}_s - x_{\min}}{x_{\max} - x_{\min}} \times \pi \quad (21)$$

where x_{\min} and x_{\max} denote the minimum and maximum values found across all elements in all vectors within the input data set, and PE_{\min} and PE_{\max} are the minimum and maximum values of the positional encoding data.

Different scaling treatments are applied to the positional encoding $PE_{(s)}$ and the input data \mathbf{x}_s due to the characteristics of the qubit rotation gate $R_x(\theta)$. This gate rotates the quantum state around the X axis by an angle θ in a counterclockwise direction, where the effective range of θ is $[0, 2\pi]$, representing a complete cycle. For the periodic $PE_{(s)}$, its period naturally matches the 2π cycle of the R_x gate. Therefore, we ensure that the values of $PE_{(s)}$ are transformed into the $[0, 2\pi]$ range through appropriate scaling to be consistent with the operational cycle of the R_x gate. However, for the original input data \mathbf{x}_s , since it does not possess periodicity, scaling it directly to $[0, 2\pi]$ might result in unintended changes in physical properties. Specifically, the encoded quantum state $R_x(2\pi - x'_s) = -ZR_x(x'_s)Z$ demonstrates a specific transformation relationship, which does not exist in the original data \mathbf{x}_s . Therefore, this step emphasizes the specific considerations that need to be taken when handling different types of data in the quantum encoding process, to ensure that the physical significance and the encoding effectiveness of the data are appropriately reflected. Through this refined data processing and using the same single qubit gates with traditional data and positional information, we are able to more effectively transform classical information into states in a quantum circuit.

3.4. Loss Function

We train our model on the dataset $\mathcal{D} = \{(\mathbf{x}_{m;1}, \mathbf{x}_{m;2}, \dots, \mathbf{x}_{m;S_m}), y_m\}_{m=1}^{N_s}$ by minimizing the loss function, where N_s represents the total number of samples, and the label $\bar{y}_m \in \{0, 1\}$ for each sample indicates its category.

For each sample, S_m denotes the number of words it contains, and each input data $\mathbf{x}_{m,s}$ is an n -dimensional vector.

The feature vector for each sample is obtained by summing and averaging the outputs $y_{m,s}$, where $1 \leq m \leq N_s$ and $1 \leq s \leq S_m$:

$$\mathbf{y}_m = \frac{1}{S_m} \sum_{s=1}^{S_m} \mathbf{y}_{m,s} \quad (22)$$

The output \mathbf{y}_m of each sample is input into a fully connected layer to produce the binary prediction value \hat{y}_m for each sample:

$$\hat{y}_m := \sigma(\mathbf{w}^\top \cdot \mathbf{y}_m + b) \quad (23)$$

where \mathbf{w} and b represent the weight and bias of the fully connected layer, respectively, and σ denotes the sigmoid activation function.

For classification problems, there are many loss functions to choose from, such as cross-entropy loss and mean squared error (L2 loss). In the current work, we use the simple and effective mean squared error as the loss function:

$$\mathcal{L}(\Theta, \mathbf{w}, b; \mathcal{D}) = \frac{1}{2N_s} \sum_{m=1}^{N_s} (\hat{y}_m - \bar{y}_m)^2 \quad (24)$$

where Θ represents all trainable parameters in the ansatz.

Algorithm 1 QMSAN training algorithm.

Input: Batch sizes **BS**. Number of words per sample S_m . Learning rate η . Number of quantum embedding Layers L . Number of qubits n . The scaled position encodings t_s . The scaled training data set $\mathcal{D} = (\mathbf{x}'_{m;1}, \mathbf{x}'_{m;2}, \dots, \mathbf{x}'_{m;S_m}), y_m\}_{m=1}^{N_s}$. $\Theta \sim \mathcal{N}(0, 0.01)$, $\mathbf{w} \sim \mathcal{N}(0, 0.01)$, $b \leftarrow 0$

- 1: **repeat**
- 2: **for** m from 1 to **BS** **do**
- 3: **for** s from 1 to S_m **do**
- 4: $\rho_{s,q} \leftarrow \text{tr}_B(U_{\text{emb}}(\mathbf{x}'_s, \mathbf{t}_s, \theta_q, L) |0\rangle^{\otimes n} \langle 0|^{\otimes n} U_{\text{emb}}^\dagger(\mathbf{x}'_s, \mathbf{t}_s, \theta_q, L))$
- 5: $\rho_{s,k} \leftarrow \text{tr}_B(U_{\text{emb}}(\mathbf{x}'_s, \mathbf{t}_s, \theta_k, L) |0\rangle^{\otimes n} \langle 0|^{\otimes n} U_{\text{emb}}^\dagger(\mathbf{x}'_s, \mathbf{t}_s, \theta_k, L))$
- 6: $|x_{s,v}\rangle \leftarrow U_{\text{emb}}(\mathbf{x}'_s, \mathbf{t}_s, \theta_v, L) |0\rangle^{\otimes n}$
- 7: $\mathbf{v}_s \leftarrow [\langle Z_1 \rangle_s \quad \langle Z_2 \rangle_s \quad \dots \quad \langle Z_n \rangle_s]^\top$
- 8: **end for**
- 9: $\mathbf{y}_m \leftarrow \text{QAttention}(\rho_q, \sigma_k, \mathbf{v})$
- 10: $\hat{y}_m := \sigma(\mathbf{w}^\top \cdot \mathbf{y}_m + b)$
- 11: **end for**
- 12: $\mathcal{L} \leftarrow \frac{1}{2N_s} \sum_{m=1}^{N_s} (\hat{y}_m - \bar{y}_m)^2$
- 13: $\Theta \leftarrow \Theta - \eta \nabla_{\Theta} \mathcal{L}$
- 14: $\mathbf{w} \leftarrow \mathbf{w} - \eta \nabla_{\mathbf{w}} \mathcal{L}$
- 15: $b \leftarrow b - \eta \nabla_b \mathcal{L}$
- 16: **until** converged

Output: Optimal parameters $\Theta^*, \mathbf{w}^*, b^*$

4. NUMERICAL EXPERIMENTS

In this section, we present simulation experiments for text classification tasks conducted on the Tensorcircuit platform [59]. These experiments aimed

to evaluate our model’s effectiveness in processing various types and sizes of text data, as well as its robustness to noise perturbations. For this purpose, we selected two types of publicly available datasets to validate the efficacy of our model. The first type consists of simple sentences or phrases, aiming to evaluate the model’s performance in understanding sentence meaning and grammatical structure. This type includes the MC and RP datasets [60]. The second type, known as the Sentiment Labelled Sentences Data Set [61], comprises three subsets of real-world user reviews. It is primarily used to assess the model’s ability to analyze sentence sentiment, including the Yelp, IMDb, and Amazon datasets. The study first evaluated models without position encoding information on both types of datasets. Subsequently, an in-depth analysis was conducted on models integrated with position encoding information on the second type of dataset. Considering that it is impossible to completely eliminate noise in practical noisy intermediate-scale quantum (NISQ) devices, the model is affected by various errors. This research simulated the impact of three types of noise: depolarizing, phase-damping, and amplitude-damping on model results in a simulation environment to evaluate the model’s robustness to noise.

4.1. Datasets

- In the MC (Meaning Classification) task, there are 130 sentences (70 train + 30 development + 30 test), each with 3 or 4 words. Half of the sentences are related to food, and the other half to information technology (IT). The task’s vocabulary consists of 17 words, with some words shared between the two categories, making this task challenging [60].
- In the RP (RELPRON) task, there are 105 noun phrase sentences containing relative clauses (74 train + 31 test), each with 4 words. The task’s vocabulary has 115 words, and the selection of phrases ensures that each word appears at least three times in the dataset. The goal is to determine whether a noun phrase contains a subject or object relative clause. Compared to the MC task, the larger vocabulary and resulting word sparsity make this task a more challenging benchmark [60].
- The Sentiment Labelled Sentences dataset comprises reviews from three websites: Amazon, IMDb, and Yelp, with each website providing 1000

sentences labeled with sentiments. The sentences in this dataset have an average length of 10.2 words, with the shortest sentence being 1 word and the longest being 30 words. The IMDb dataset contains movie reviews from the imdb.com website, with an average sentence length of 14.4 words. The shortest sentence in this dataset is 1 word, and the longest is 71 words. The Yelp dataset consists of restaurant reviews, with an average sentence length of 10.9 words, a minimum of 1 word, and a maximum of 32 words. In all datasets, reviews with scores of 4 and 5 are considered positive, while those with scores of 1 and 2 are considered negative. In each subset, positive and negative sentiment reviews each account for 50%. The datasets randomly select 80% of the data as the training set and the remaining 20% as the test set.

4.2. Experiment Settings

Table 1: Experimental configuration. ‘LR’ denotes learning rate. ‘-P’ for models with quantum position encoding and ‘-NP’ for models without it.

Data set	n	L	LR-NP			LR-P		
			ENN-NP	CB-NP	AA-NP	ENN-P	CB-P	AA-P
MC	2	1	0.005	0.006	0.009	/	/	/
RP	4	2	0.002	0.05	0.01	/	/	/
IMDb	4	1	0.008	0.008	0.01	0.008	0.008	0.008
Yelp	4	1	0.007	0.007	0.03	0.03	0.03	0.01
Amazon	4	1	0.08	0.009	0.09	0.02	0.01	0.02

To fairly compare our experimental results with those in Ref.[38], we set the number of qubits for the input of quantum embeddings to be the same as theirs. Specifically, we used $n = 2$ qubits for the MC task and $n = 4$ qubits for the other tasks. The detailed hyperparameter settings are shown in Table 1.

To explore the potential advantages of our qubit topology in QMSAN, we compared three distinct entanglement schemes within the quantum embeddings module: Extended Nearest-neighbor (ENN) ansatz, circuit-block (CB) ansatz[62], and all-to-all (AA) ansatz[63], as shown in Fig. 2. The

CB ansatz is characterized by a looped arrangement of qubits, suitable for efficient closed-circuit operations. The Extended Nearest-Neighbor (ENN) ansatz is derived from the Nearest-Neighbor (NN) ansatz[62] to have an equivalent number of parameters as the CB ansatz, yet it introduces a different entanglement strategy. This variation allows for the experimental comparison of outcomes resulting from different entanglement approaches. In contrast, the AA ansatz is based on a fully connected network of qubits, allowing for direct interactions between any pair of qubits and resulting in enhanced entanglement potential.

For clarity, we denote the QMSAN variants with these entanglement schemes as QMSAN-ENN, QMSAN-CB, and QMSAN-AA, respectively. Additionally, we introduce suffixes to indicate the presence or absence of our novel quantum position encoding: '-P' for models with quantum position encoding and '-NP' for models without it. For example, QMSAN-ENN-P denotes QMSAN model with ENN ansatz and position encoding, while QMSAN-ENN-NP denotes the variant without position encoding.

Furthermore, we propose a variant called QMSAN-D 2π , where the input data is scaled to the range $[0, 2\pi]$. This variant serves as a comparison model to assess the impact of different scaling approaches on the performance of our quantum embeddings. Similarly, we propose the Quantum Pure-State Attention Network (QPSAN) to compare different computational methods for quantum queries and keys. QPSAN employs a distinct method for computing the similarity between quantum queries and keys by utilizing the inner product of pure states. Apart from this, QPSAN and QMSAN maintain identical structures. To facilitate comparisons, we adopt the same naming convention for QPSAN and QMSAN-D 2π variants, such as QPSAN-ENN-P and QMSAN-D 2π -ENN-P.

Assuming the quantum embeddings ansatz has n qubits and L layers, the AA ansatz has $3n((n-1)/2+n)L$ parameters, while both the ENN and CB ansatzes have $6nL$ parameters. The ansatzes for queries, keys, and values have the same depth. Notably, the AA ansatz has an increased total number of two-qubit gates compared to the ENN and CB ansatzes, providing it with stronger entanglement capabilities.

All ansatzes parameters Θ and the weights \mathbf{w} of the classical part of the network are initialized from a normal distribution with mean 0 and variance 0.1. The bias b of the classical network is initialized to 0. For the value ansatz, we measure the expectation value under the Pauli- Z observable. For the attention matrix, we measure the probability of the output state $|0\rangle$ under

the Pauli- Z observable. Through these measurements, we convert quantum data into classical data that can be utilized by subsequent classical networks. In our work, we use the Tensorcircuit framework[59] for simulating quantum circuits and the Tensorflow[64] framework for parameter optimization, with the optimizer Adam [65]. The batch size is 64, and training stops when convergence is reached or after a fixed number of epochs. In the MC and RP tasks, we repeat each experiment 9 times with different parameter initializations. For the Sentiment Labelled Sentences Data Set task, we use cross-validation for the experiments.

4.3. Experiments with Non-Positional Models

In this experiment, we conduct numerical experiments with two model architectures: Non-Positional Models and Positional Models. This allows us to deeply analyze the performance differences between models and explore how positional information enhances the model’s understanding and processing of data. The experimental design aims to compare with representative models in classical networks and quantum networks. For the MC and RP datasets, we compare our experimental results with a classical quantum model based on syntactic analysis [60] and further with QSANN. Meanwhile, for three public sentiment analysis datasets (Yelp, IMDB, and Amazon), our models will be compared and analyzed with classical self-attention neural networks (CSANN) [38] and QSANN models. Through these comparative experiments, we aim to comprehensively evaluate the performance and potential of quantum self-attention networks across different models and datasets.

Table 2: Test accuracy of our proposed methods compared to DisCoCat and CSANN on MC and RP task.

Method	MC			RP		
	#Paras	TrainAcc(%)	TestAcc(%)	#Paras	TrainAcc(%)	TestAcc(%)
DisCoCat[60]	40	83.10	79.80	168	90.60	72.30
QSANN [38]	25	100.00	100.00	109	95.35	67.74
QPSAN-ENN-NP	15	100.00	100.00	53	95.95	70.97
QPSAN-CB-NP	15	100.00	100.00	53	95.95	70.97
QPSAN-AA-NP	18	100.00	100.00	137	95.95	74.19
QMSAN-ENN-NP	15	100.00	100.00	53	95.95	74.19
QMSAN-CB-NP	15	100.00	100.00	53	95.95	74.19
QMSAN-AA-NP	18	100.00	100.00	137	97.30	77.42

Table 3: Test accuracy of our proposed methods compared to CSANN and the naive method on Yelp, IMDb, and Amazon data sets.

Method	Yelp			IMDb			Amazon		
	#Paras	TrainAcc(%)	TestAcc(%)	#Paras	TrainAcc(%)	TestAcc(%)	#Paras	TrainAcc(%)	TestAcc(%)
CSANN[38]	785	/	83.11 ± 0.89	785	/	79.67 ± 0.83	785	/	83.22 ± 1.28
QSANN[38]	49	/	84.79 ± 1.29	49	/	80.28 ± 1.78	61	/	84.25 ± 1.75
QMSAN-ENN-NP	29	99.53 ± 0.22	84.14 ± 2.27	29	99.48 ± 0.37	84.12 ± 2.31	29	99.80 ± 0.10	86.72 ± 2.38
QMSAN-CB-NP	29	99.58 ± 0.23	84.40 ± 1.98	29	99.45 ± 0.24	83.74 ± 2.01	29	99.83 ± 0.17	86.61 ± 1.71
QMSAN-AA-NP	71	99.65 ± 0.18	84.73 ± 2.34	71	99.50 ± 0.40	83.76 ± 3.04	71	99.75 ± 0.18	86.56 ± 1.90
QMSAN-ENN-P	29	99.45 ± 0.32	84.85 ± 1.33	29	99.18 ± 0.41	84.77 ± 3.12	29	99.87 ± 0.94	87.41 ± 1.16
QMSAN-CB-P	29	99.80 ± 0.20	84.82 ± 1.21	29	99.18 ± 0.41	84.82 ± 2.96	29	99.90 ± 0.93	87.43 ± 1.16
QMSAN-AA-P	71	99.55 ± 0.26	84.96 ± 3.34	71	99.33 ± 0.36	84.29 ± 2.32	71	99.91 ± 0.50	87.48 ± 1.02

MC dataset. We first conducted experiments on models without positional information, and the results are detailed in Table 2. On the MC dataset, the QMSAN-NP series models, regardless of the entanglement structure used, can perfectly distinguish sentences related to food and information technology, significantly outperforming the quantum model based on syntactic analysis mentioned in reference [60]. Since the task of the MC dataset is relatively simple, different entanglement structures can effectively capture the semantic information of sentences in this case. Notably, in terms of the number of parameters, QMSAN-NP series models use fewer parameters compared to the QSANN and classical deep learning model DisCoCat, yet achieve the same performance level, indicating the potential application value of QMSAN-NP series models in resource-limited environments.

RP dataset. For the RP dataset, we evaluate the model’s performance in processing more complex data. The experimental results Table 2 show different degrees of performance on different variants of the QMSAN-NP series models, with the QMSAN-AA-NP model performing the best with a test accuracy of 77.42%. The experimental results of the other two entanglement structures are reduced, which may be because the fully connected structure provides more abundant information entanglement, helping the model better capture complex relationships in sentences. The experimental results of different series models of QMSAN-NP all surpass the 72.30% test accuracy of DisCoCat based on syntactic analysis and significantly outperform the 67.74% of the QSANN model. Although the complexity of the RP dataset is significantly higher than that of the MC dataset, our model can still effectively parse and infer complex relationships in the dataset, further confirming the great potential of quantum self-attention networks in enhancing the model’s understanding ability. Specifically, our QMSAN-ENN-NP and

QMSAN-CB-NP maintain a lower number of parameters and computational cost while improving performance, indicating the potential of QMSAN models in handling natural language processing tasks with certain complexity.

Concurrently, we conducted a comparative analysis of the experimental outcomes for QMSAN-NP and QPSAN-NP on this dataset. The QMSAN-NP series models’ performance on the RP dataset is superior to that of the QPSAN-NP series models, with QMSAN-AA-NP model achieving the highest test accuracy of 77.42%, 3.23% higher than the highest test accuracy of 74.19% of the QPSAN-NP series models. The specific results are shown in Table 2. This indicates that QMSAN model can more accurately capture the similarity features between queries and keys using the mixed state approach, especially in processing complex semantic relationships. This validates our theoretical analysis in Section 3.2.

Sentiment Labelled Sentences Data Set. This part of the research focuses on the Sentiment Labelled Sentences Data Set, covering more complex and diverse sentiment analysis tasks. The Sentiment Labelled Sentences Data Set, which includes three subsets: Yelp, IMDb, and Amazon, covers different review categories, each with its unique language usage and emotional expression, increasing the difficulty and complexity of sentiment analysis and providing a broader and more challenging testing platform for our QMSAN-NP series models. The experimental results are detailed in Table 3.

Compared to classical model CSANN, the QMSAN-NP series models’ methods have achieved comprehensive improvements in accuracy, with the maximum being 4.45% on IMDb for QMSAN-ENN-NP. Compared to the quantum model QSANN, the accuracy has significantly improved on most datasets, with the maximum increase of 3.84% on the IMDb dataset and 2.47% on the Amazon dataset. The accuracy on the Yelp dataset is also similar, indicating that QMSAN-NP series models, by using mixed-state quantum attention calculation and trainable embedded quantum modules, can more effectively capture the intrinsic features and complex relationships of data, providing a richer data representation for complex sentiment analysis tasks, thereby improving the model’s representational ability. It can effectively adapt to sentiment classification tasks in different domains and data distributions, not only significantly improving performance in most datasets but also maintaining stable performance in different application scenarios, demonstrating better generalization ability.

For the number of parameters, QMSAN-ENN-NP and QMSAN-CB-NP

have 29 parameters, significantly fewer than CSANN’s 785 and QSANN’s 49, yet they show noticeable performance improvements on most datasets. Being able to capture sufficient information with fewer parameters is very beneficial for reducing computational resources and improving efficiency. This indicates that our model has a clear advantage in capturing emotional features in textual data. Among the three QMSAN-NP series models, QMSAN-AA-NP has slightly more parameters and stronger quantum entanglement capabilities, but it only has a slightly higher test accuracy on the Yelp dataset compared to the other two models. This suggests that these more complex different datasets may require different entanglement methods.

4.4. Experiments with Positional Models

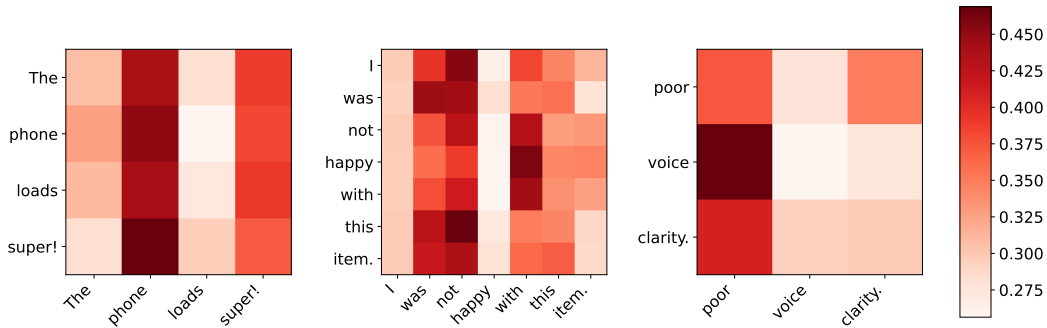


Figure 5: Heat maps of quantum self-attention.

To further enhance model performance, this section of the experiment focuses on analyzing the impact of positional information on QMSAN model. Considering the importance of positional information in text sequence processing, we adopted the use of fixed quantum gates to encode positional information. Since the average number of words per sentence in the MC and RP datasets is relatively small, the impact of positional information on model performance may not be significant. Therefore, we chose to evaluate the performance of the QMSAN series models with introduced positional information on the Yelp, IMDb, and Amazon data subsets to more accurately measure the impact of positional information. Experiments show that the QMSAN-P series models with fixed positional information have comprehensively improved performance compared to models without positional information. The experimental results are detailed in Table 3, with the maximum increase in test accuracy of 0.71% on the Yelp dataset, 1.08% on the

IMDb dataset, and 0.92% on the Amazon dataset. In addition, we provide attention heat maps of the data, which visually illustrate the effectiveness of our method as shown in the Fig. 5.

The above experimental results show that our method can effectively encode positional information in text sequences, comprehensively improving the accuracy of QMSAN model in different sentiment analysis tasks. By using fixed quantum gates with positional information, the model is provided with key information about the relative positions of words in the text, enhancing the understanding of the entire text structure. The advantage of this method is that it provides a fixed and efficient way for quantum models to incorporate positional information. We do not need to increase additional qubits resources and do not need to add trainable parameters, which can save computational resources and time during training. Moreover, since a stable and consistent way is adopted to represent the positional information of words, this helps the model to generalize better to unseen data.

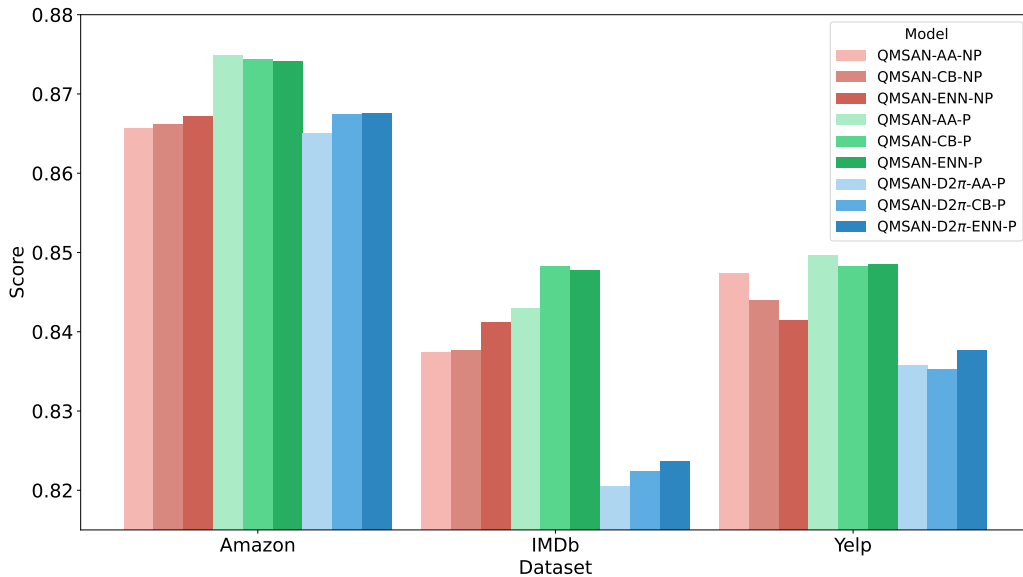


Figure 6: Test accuracy of different forms of data scaling methods.

At the same time, we compared the experiments of the QMSAN-D2π-P series models, which scale the input data to $[0, 2\pi]$. The results, as shown in Fig. 6, indicate that the test accuracy of the QMSAN-D2π-P series models is comprehensively lower than that of the QMSAN-P series models, and even

lower than the performance of QMSAN-NP without positional information on some datasets. This also supports our approach to scaling traditional data and positional encoding information, as analyzed in Section 3.3.

4.5. Noise robustness

In the practical application of quantum computing, the impact of quantum noise is a significant factor, as NISQ is sensitive to the environment and susceptible to noise interference. To evaluate the robustness of our QMSAN-P series models in a quantum noise environment, we conducted a series of experiments using the Tensorcircuit simulation software. We considered not only common noise channels such as depolarizing noise, amplitude damping noise, and phase damping noise but also explored the impact of different Ansatz structures on noise resistance.

Depolarizing channel (DP) causes a qubit to depolarize with probability p . For a single qubit, it is replaced by the completely mixed state $I/2$, and remains unchanged with probability $1-p$. The depolarizing channel can be represented as the following density matrix mapping:

$$\varepsilon_{\text{DP}}(\rho) = (1 - p)\rho + \frac{p}{3}(X\rho X + Y\rho Y + Z\rho Z) \quad (25)$$

where ρ is the original density matrix, and X, Y, Z are Pauli matrices.

Amplitude damping (AD) describes the process of a quantum system losing energy, while phase damping (PD) describes the process of a quantum system losing phase information without losing energy. The noise mapping for a single qubit’s density matrix can be uniformly expressed as:

$$\varepsilon_{\text{AD/PD}}(\rho) = E_0\rho E_0^\dagger + E_1\rho E_1^\dagger \quad (26)$$

where for amplitude damping, $E_0 = |0\rangle\langle 0| + \sqrt{1-p}|1\rangle\langle 1|$ and $E_1 = \sqrt{p}|0\rangle\langle 1|$, and for phase damping, $E_0 = |0\rangle\langle 0| + \sqrt{1-p}|1\rangle\langle 1|$ and $E_1 = \sqrt{p}|1\rangle\langle 1|$. E_0 and E_1 represent Kraus operators, and p represents the noise level.

We added these single-qubit noise channels to the embedding layer circuit for noise addition. At noise levels of 0.01, 0.1, and 0.2, the experimental results are shown in Table 4. The performance of the QMSAN-P series models showed a slight decline, with the maximum accuracy drop of 1.54% on the Yelp dataset under the PD(0.1) noise model. The maximum accuracy drop on the IMDb dataset was 1.48% under the DP(0.2) noise model, and the maximum accuracy drop on the Amazon dataset was 1.38% under the

Table 4: Test accuracy of QMSAN-P series models on Yelp, IMDb, and Amazon data sets with different noise models. DP denotes Depolarizing channel, AD denotes Amplitude damping, and PD denotes Phase damping.

Noise Model	Yelp			IMDb			Amazon		
	ENN-P	CB-P	AA-P	ENN-P	CB-P	AA-P	ENN-P	CB-P	AA-P
DP(0.01)	84.55±1.79	84.51±1.38	84.77±1.81	84.10±3.14	84.27±2.16	83.89±3.64	86.97±1.66	86.98±1.53	86.40±1.16
DP(0.1)	84.49±1.59	84.13±2.27	84.11±2.35	84.30±1.81	84.03±2.07	83.58±1.58	87.02±0.71	86.87±1.21	87.23±1.40
DP(0.2)	83.97±1.74	83.76±3.66	84.22±2.34	83.29±3.04	83.80±1.63	83.83±2.66	86.17±1.53	86.05±1.97	86.33±1.50
AD(0.01)	84.53±2.28	83.99±0.97	84.63±1.39	84.01±3.02	84.17±3.12	83.77±2.42	86.42±1.02	87.34±1.17	87.21±1.81
AD(0.1)	84.05±2.30	84.15±2.01	84.54±1.87	84.09±2.59	83.98±3.89	83.69±1.69	86.30±0.51	87.29±0.81	86.99±2.25
AD(0.2)	83.87±1.40	83.67±1.71	84.20±1.86	83.95±2.54	84.07±2.70	83.91±1.71	86.33±2.29	86.23±1.63	87.30±1.72
PD(0.01)	84.11±2.56	84.60±1.83	83.90±1.53	84.02±2.79	84.02±2.79	84.05±2.43	87.02±0.95	86.78±0.75	87.05±1.05
PD(0.1)	84.35±2.73	84.22±2.82	83.42±1.32	84.22±2.73	83.93±2.08	83.94±3.22	86.37±1.96	86.32±1.96	86.86±2.25
PD(0.2)	84.33±1.44	84.46±1.24	83.85±1.33	83.66±2.58	84.11±2.99	83.71±4.06	86.91±2.15	86.83±1.69	86.89±2.36

DP(0.2) noise model. The decrease in test accuracy caused by noise did not exceed 1.6%, indicating that the QMSAN series models can maintain high performance stability in a low-level quantum noise environment, showing good robustness to common quantum noise, and validating the feasibility of running QMSAN models in a real quantum computing environment.

5. CONCLUSION

This paper proposes a novel Quantum Multi-head Self-Attention Network (QMSAN) model, combining the characteristics of quantum computing with the advantages of classical self-attention networks to enhance the processing capabilities and efficiency of NLP tasks. Our model operates on queries and keys under mixed states through quantum gate operations and directly generates similarity scalars through measurement. Compared to conventional pure state unitary transformations, our method expands the expressive power of the quantum system through mixed state operations, enabling the model to capture the similarity between queries and keys more comprehensively and finely. We also introduced a trainable quantum embedding module that maps classical data to quantum states, achieving more efficient data representation and processing. Additionally, we proposed a novel quantum positional encoding scheme, which encodes positional information by introducing additional fixed quantum gates in the quantum circuit, improving the accuracy of encoding without increasing additional qubits resources.

The experimental results on various datasets verify the effectiveness of QMSAN. Compared to classical self-attention networks, our model not only significantly reduces the number of parameters under the same input sequence conditions but also demonstrates superior performance, proving its

better learning ability. We anticipate that future work will further explore the potential of quantum machine learning models, realizing a fully quantum self-attention network model, and fully utilizing the unique advantages of quantum computing. It serves as a scalable module, facilitating the construction of quantum versions of the Transformer architecture, thereby bringing unprecedented computational power and efficiency to machine learning.

Acknowledgments

The present work is supported by Education and Scientific Research Project for Young and Middle-aged Teachers of Fujian Province, China (Grant numbers JAT200499) and the Science and Technology Development Fund, Macau SAR (Grant numbers 0093/2022/A2, 0076/2022/A2, and 0008/2022/AGJ)

References

- [1] N. Lambert, Y.-N. Chen, Y.-C. Cheng, C.-M. Li, G.-Y. Chen, F. Nori, Quantum biology, *Nature Physics* 9 (1) (2013) 10–18.
- [2] F. Xu, X. Ma, Q. Zhang, H.-K. Lo, J.-W. Pan, Secure quantum key distribution with realistic devices, *Reviews of Modern Physics* 92 (2) (2020) 025002.
- [3] N. Gisin, R. Thew, Quantum communication, *Nature photonics* 1 (3) (2007) 165–171.
- [4] J. Biamonte, P. Wittek, N. Pancotti, P. Rebentrost, N. Wiebe, S. Lloyd, Quantum machine learning, *Nature* 549 (7671) (2017) 195–202.
- [5] M. Schuld, I. Sinayskiy, F. Petruccione, An introduction to quantum machine learning, *Contemporary Physics* 56 (2) (2015) 172–185.
- [6] M. Schuld, N. Killoran, Quantum machine learning in feature hilbert spaces, *Physical Review Letters* 122 (4) (2019) 040504.
- [7] P. Wittek, *Quantum machine learning: what quantum computing means to data mining*, Academic Press, 2014.
- [8] Y. LeCun, L. Bottou, Y. Bengio, P. Haffner, Gradient-based learning applied to document recognition, *Proceedings of the IEEE* 86 (11) (1998) 2278–2324.

- [9] J. L. Elman, Finding structure in time, *Cognitive Science* 14 (2) (1990) 179–211.
- [10] Y. Kim, Convolutional neural networks for sentence classification, *arXiv:1408.5882* (2014).
- [11] S. Lai, L. Xu, K. Liu, J. Zhao, Recurrent convolutional neural networks for text classification, in: *Proceedings of the AAAI Conference on Artificial Intelligence*, Vol. 29, 2015.
- [12] Y. Cheng, L. Yao, G. Xiang, G. Zhang, T. Tang, L. Zhong, Text sentiment orientation analysis based on multi-channel cnn and bidirectional gru with attention mechanism, *IEEE Access* 8 (2020) 134964–134975.
- [13] A. Hassan, A. Mahmood, Convolutional recurrent deep learning model for sentence classification, *IEEE Access* 6 (2018) 13949–13957.
- [14] S. Liu, N. Yang, M. Li, M. Zhou, A recursive recurrent neural network for statistical machine translation, in: *Proceedings of the 52nd Annual Meeting of the Association for Computational Linguistics (Volume 1: Long Papers)*, 2014, pp. 1491–1500.
- [15] T. He, X. Tan, Y. Xia, D. He, T. Qin, Z. Chen, T.-Y. Liu, Layer-wise coordination between encoder and decoder for neural machine translation, *Advances in Neural Information Processing Systems* 31 (2018).
- [16] A. Vaswani, N. Shazeer, N. Parmar, J. Uszkoreit, L. Jones, A. N. Gomez, Ł. Kaiser, I. Polosukhin, Attention is all you need, *Advances in Neural Information Processing Systems* 30 (2017).
- [17] A. Radford, K. Narasimhan, T. Salimans, I. Sutskever, et al., Improving language understanding by generative pre-training (2018).
- [18] J. Achiam, S. Adler, S. Agarwal, L. Ahmad, I. Akkaya, F. L. Aleman, D. Almeida, J. Altenschmidt, S. Altman, S. Anadkat, et al., Gpt-4 technical report, *arXiv:2303.08774* (2023).
- [19] X. Qiu, T. Sun, Y. Xu, Y. Shao, N. Dai, X. Huang, Pre-trained models for natural language processing: A survey, *Science China Technological Sciences* 63 (10) (2020) 1872–1897.

- [20] X. Wang, T. Gao, Z. Zhu, Z. Zhang, Z. Liu, J. Li, J. Tang, Kepler: A unified model for knowledge embedding and pre-trained language representation, *Transactions of the Association for Computational Linguistics* 9 (2021) 176–194.
- [21] A. Haleem, M. Javaid, R. P. Singh, An era of chatgpt as a significant futuristic support tool: A study on features, abilities, and challenges, *BenchCouncil Transactions on Benchmarks, Standards and Evaluations* 2 (4) (2022) 100089.
- [22] B. Min, H. Ross, E. Sulem, A. P. B. Veyseh, T. H. Nguyen, O. Sainz, E. Agirre, I. Heintz, D. Roth, Recent advances in natural language processing via large pre-trained language models: A survey, *ACM Computing Surveys* 56 (2) (2023) 1–40.
- [23] F. Liu, G. Li, Y. Zhao, Z. Jin, Multi-task learning based pre-trained language model for code completion, in: *Proceedings of the 35th IEEE/ACM International Conference on Automated Software Engineering*, 2020, pp. 473–485.
- [24] X. Han, Z. Zhang, N. Ding, Y. Gu, X. Liu, Y. Huo, J. Qiu, Y. Yao, A. Zhang, L. Zhang, et al., Pre-trained models: Past, present and future, *AI Open* 2 (2021) 225–250.
- [25] X. Zhu, J. Li, Y. Liu, C. Ma, W. Wang, A survey on model compression for large language models, *arXiv:2308.07633* (2023).
- [26] S. Zhu, T. Yu, T. Xu, H. Chen, S. Dustdar, S. Gigan, D. Gunduz, E. Hosain, Y. Jin, F. Lin, et al., Intelligent computing: the latest advances, challenges, and future, *Intelligent Computing* 2 (2023) 0006.
- [27] M.-H. Yung, Quantum supremacy: some fundamental concepts, *National Science Review* 6 (1) (2019) 22–23.
- [28] A. W. Harrow, A. Montanaro, Quantum computational supremacy, *Nature* 549 (7671) (2017) 203–209.
- [29] M. Cerezo, G. Verdon, H.-Y. Huang, L. Cincio, P. J. Coles, Challenges and opportunities in quantum machine learning, *Nature Computational Science* 2 (9) (2022) 567–576.

- [30] M. Schuld, N. Killoran, Is quantum advantage the right goal for quantum machine learning?, *Prx Quantum* 3 (3) (2022) 030101.
- [31] M. Schuld, Supervised quantum machine learning models are kernel methods, *arXiv:2101.11020* (2021).
- [32] Y. Liu, S. Arunachalam, K. Temme, A rigorous and robust quantum speed-up in supervised machine learning, *Nature Physics* 17 (9) (2021) 1013–1017.
- [33] A. J. Daley, I. Bloch, C. Kokail, S. Flannigan, N. Pearson, M. Troyer, P. Zoller, Practical quantum advantage in quantum simulation, *Nature* 607 (7920) (2022) 667–676.
- [34] M. Abbaszade, V. Salari, S. S. Mousavi, M. Zomorodi, X. Zhou, Application of quantum natural language processing for language translation, *IEEE Access* 9 (2021) 130434–130448.
- [35] Y. Li, Z. Wang, R. Han, S. Shi, J. Li, R. Shang, H. Zheng, G. Zhong, Y. Gu, Quantum recurrent neural networks for sequential learning, *arXiv:2302.03244* (2023).
- [36] S. Y.-C. Chen, S. Yoo, Y.-L. L. Fang, Quantum long short-term memory, in: *ICASSP 2022-2022 IEEE International Conference on Acoustics, Speech and Signal Processing (ICASSP)*, IEEE, 2022, pp. 8622–8626.
- [37] L. Bi-Directional, Mechanism for sentence modeling, in: *Neural Information Processing: 24th International Conference, ICONIP 2017, Guangzhou, China, November 14-18, 2017, Proceedings, Part II, Vol. 10635*, Springer, 2017, p. 178.
- [38] G. Li, X. Zhao, X. Wang, Quantum self-attention neural networks for text classification, *Science China Information Sciences* 67 (4) (2024) 1–13.
- [39] R.-x. Zhao, J. Shi, S. Zhang, X. Li, Qsan: A near-term achievable quantum self-attention network, *arXiv:2207.07563* (2022).
- [40] R.-X. Zhao, J. Shi, X. Li, Qksan: A quantum kernel self-attention network, *arXiv:2308.13422* (2023).

- [41] M. A. Nielsen, I. L. Chuang, Quantum computation and quantum information, Cambridge University Press, 2010.
- [42] I. Cong, S. Choi, M. D. Lukin, Quantum convolutional neural networks, *Nature Physics* 15 (12) (2019) 1273–1278.
- [43] M. Schuld, A. Bocharov, K. M. Svore, N. Wiebe, Circuit-centric quantum classifiers, *Physical Review A* 101 (3) (2020) 032308.
- [44] M. Ostaszewski, L. M. Trenkwalder, W. Masarczyk, E. Scerri, V. Dunjko, Reinforcement learning for optimization of variational quantum circuit architectures, *Advances in Neural Information Processing Systems* 34 (2021) 18182–18194.
- [45] M. Ostaszewski, E. Grant, M. Benedetti, Structure optimization for parameterized quantum circuits, *Quantum* 5 (2021) 391.
- [46] M. Schuld, R. Sweke, J. J. Meyer, Effect of data encoding on the expressive power of variational quantum-machine-learning models, *Physical Review A* 103 (3) (2021) 032430.
- [47] S. Lloyd, M. Schuld, A. Ijaz, J. Izaac, N. Killoran, Quantum embeddings for machine learning, *arXiv:2001.03622* (2020).
- [48] G. Li, R. Ye, X. Zhao, X. Wang, Concentration of data encoding in parameterized quantum circuits, *Advances in Neural Information Processing Systems* 35 (2022) 19456–19469.
- [49] A. Shrestha, A. Mahmood, Review of deep learning algorithms and architectures, *IEEE access* 7 (2019) 53040–53065.
- [50] Y. Chen, H. Jiang, C. Li, X. Jia, P. Ghamisi, Deep feature extraction and classification of hyperspectral images based on convolutional neural networks, *IEEE Transactions on Geoscience and Remote Sensing* 54 (10) (2016) 6232–6251.
- [51] P. J. Coles, M. Cerezo, L. Cincio, Strong bound between trace distance and hilbert-schmidt distance for low-rank states, *Physical Review A* 100 (2) (2019) 022103.
- [52] J. C. Garcia-Escartin, P. Chamorro-Posada, Swap test and hong-ou-mandel effect are equivalent, *Physical Review A* 87 (5) (2013) 052330.

- [53] H. Kobayashi, K. Matsumoto, T. Yamakami, Quantum merlin-arthur proof systems: Are multiple merlins more helpful to arthur?, in: Algorithms and Computation: 14th International Symposium, ISAAC 2003, Kyoto, Japan, December 15-17, 2003. Proceedings 14, Springer, 2003, pp. 189–198.
- [54] M. Y. Niu, A. Zlokapa, M. Broughton, S. Boixo, M. Mohseni, V. Smelyanskiy, H. Neven, Entangling quantum generative adversarial networks, *Physical Review Letters* 128 (22) (2022) 220505.
- [55] K. Wu, H. Peng, M. Chen, J. Fu, H. Chao, Rethinking and improving relative position encoding for vision transformer, in: Proceedings of the IEEE/CVF International Conference on Computer Vision, 2021, pp. 10033–10041.
- [56] J. Su, M. Ahmed, Y. Lu, S. Pan, W. Bo, Y. Liu, Roformer: Enhanced transformer with rotary position embedding, *Neurocomputing* 568 (2024) 127063.
- [57] C. Yun, S. Bhojanapalli, A. S. Rawat, S. Reddi, S. Kumar, Are transformers universal approximators of sequence-to-sequence functions?, in: International Conference on Learning Representations, 2019.
- [58] C. Chen, Q. Zhao, Quantum generative diffusion model, *arXiv:2401.07039* (2024).
- [59] S.-X. Zhang, J. Allcock, Z.-Q. Wan, S. Liu, J. Sun, H. Yu, X.-H. Yang, J. Qiu, Z. Ye, Y.-Q. Chen, et al., Tensorcircuit: a quantum software framework for the nisq era, *Quantum* 7 (2023) 912.
- [60] R. Lorenz, A. Pearson, K. Meichanetzidis, D. Kartsaklis, B. Coecke, Qnlp in practice: Running compositional models of meaning on a quantum computer, *Journal of Artificial Intelligence Research* 76 (2023) 1305–1342.
- [61] D. Kotzias, Sentiment Labelled Sentences, UCI Machine Learning Repository, DOI: <https://doi.org/10.24432/C57604> (2015).
- [62] S. Sim, P. D. Johnson, A. Aspuru-Guzik, Expressibility and entangling capability of parameterized quantum circuits for hybrid quantum-classical algorithms, *Advanced Quantum Technologies* 2 (12) (2019) 1900070.

- [63] M. Benedetti, D. Garcia-Pintos, O. Perdomo, V. Leyton-Ortega, Y. Nam, A. Perdomo-Ortiz, A generative modeling approach for benchmarking and training shallow quantum circuits, *npj Quantum Information* 5 (1) (2019) 45.
- [64] M. Abadi, P. Barham, J. Chen, Z. Chen, A. Davis, J. Dean, M. Devin, S. Ghemawat, G. Irving, M. Isard, et al., {TensorFlow}: a system for {Large-Scale} machine learning, in: 12th USENIX Symposium on Operating Systems Design and Implementation (OSDI 16), 2016, pp. 265–283.
- [65] D. P. Kingma, J. Ba, Adam: A method for stochastic optimization, *arXiv:1412.6980* (2014).